3-D CHARACTERIZATION OF ASPHALT PAVEMENT MACROTEXTURE FOR SKID RESISTANCE EVALUATION

Y. MIAO & P. SONG
Department of Transportation Engineering, Beijing University of Technology, China
MIAOYINGHAO@BJUT.EDU.CN

ABSTRACT

This work focuses on 3-D characterization of asphalt pavement macrotexture to improve skid resistance evaluation. In situ digitizing method of asphalt pavement macrotexture is tried using a 3-D laser scanner. Field tests are conducted using the Dynamic Friction Tester (DFT), the sand patch method, and the 3-D laser scanner at 33 test sites with various highway grades and pavement types in Huairou District, Beijing, China. Three 3-D characterizing indicators are constructed using the 3-D digital macrotexture. Then, preliminary analysis is conducted to investigate the relationship of the new indicators and MTD to friction coefficient at speed of 60km/h (DFT60). The results show the 3-D characterizing indicators of macrotexture have obvious advantage over MTD in skid resistance evaluation though the indicators are not very detailed. It is necessary and possible to construct more detailed macrotexture indicators for pavement skid resistance evaluation based on the 3-D digital macrotexture in the future work.

1. INTRODUCTION

Surface texture of pavement is an important factor impacting skid resistance. It is usually divided into microtexture and macrotexture according to the wavelength and amplitude of the deviations of a pavement surface from a true planar surface with a threshold of 0.5mm [1-3]. Mean Texture Depth (MTD) and Mean Profile Depth (MPD) are usually adopted to describe macrotexture characteristics for skid resistance evaluation in practice [2,4,5]. However, it is hard to link MTD or MPD with skid resistance directly. Some studies were also conducted using multiple models and new macrotexture indicators derived from profile data [6-9]. Though the solutions are improved, they cannot fulfil the practice requirements. In fact, the macrotexture of pavement is an irregular 3-D curved surface. So, some methods for 3-D digital macrotexture collection were tried by researchers [5,9,10]. But there is no widely accepted method for practice application and there are few real 3-D characterizing macrotexture indicators.

In order to investigate the advantages of 3-D characterizing indicators of macrotexture in skid resistance evaluation, this work attempts a field digitizing method of asphalt pavement macrotexture using a 3-D laser scanner. A series of field tests are conducted using the Dynamic Friction Tester (DFT), the sand patch method, and the 3-D laser scanner. Then, some 3-D characterizing indicators of macrotexture are constructed and regression analyses are performed to relate macrotexture indicators to pavement skid resistance.

2. FIELD TESTS

With consideration of the potential differences derived from pavement types and highway grades, this work selects 5 typical asphalt pavement surfaces, including Asphalt Concrete (AC), Stone Matrix Asphalt (SMA), Rubber Asphalt Concrete (RAC), Ultra Thin Wearing Course (UTWC), and Mirco Surfacing (MS), on various grade highways in Huairou District,

Beijing, China for data collection. The field tests are conducted at 33 test sites. Table 1 lists basic information of the test sites. For convenience, each test site is coded using the highway coding, the surface type, and a sequence number such as G101-SMA-3.

Table 1 - Basic information of the test sites

Highway coding	Grade	Surface type	Number of test sites	Opening date
G101	1	SMA	5	Aug. 2010
G101	1	UTWC	4/4	Sep. 2010/Sep. 2009
G101	1	MS	4	Sep. 2009
G111	2	AC	7	Jul. 2009
G111	2	RAC	6	Sep. 2010
X020	3	AC	3	Sep. 2009

3-D digital macrotexture, friction coefficient at speed of 60km/h (DFT60), MTD are collected at each test site using 3-D laser scanner, Dynamic Friction Tester (DFT), and sand patch method respectively. The 3-D laser scanner used in this work is an EXAscan laser scanner produced by Creaform Inc. with resolution of 0.05mm and accuracy of 0.04mm. In the collection of pavement macrotexures, resolution of 0.4mm is adopted and a 100mm×100mm area is scanned for each test site. The scan result is output as an unordered point clouds file for deep analysis. Figure 1 depicts the typical 3-D digital macrotextures which are reconstructed using Geomagic Studio 12. The results of DFT60 are listed in table 2 and the results of MTD are listed in table 3.

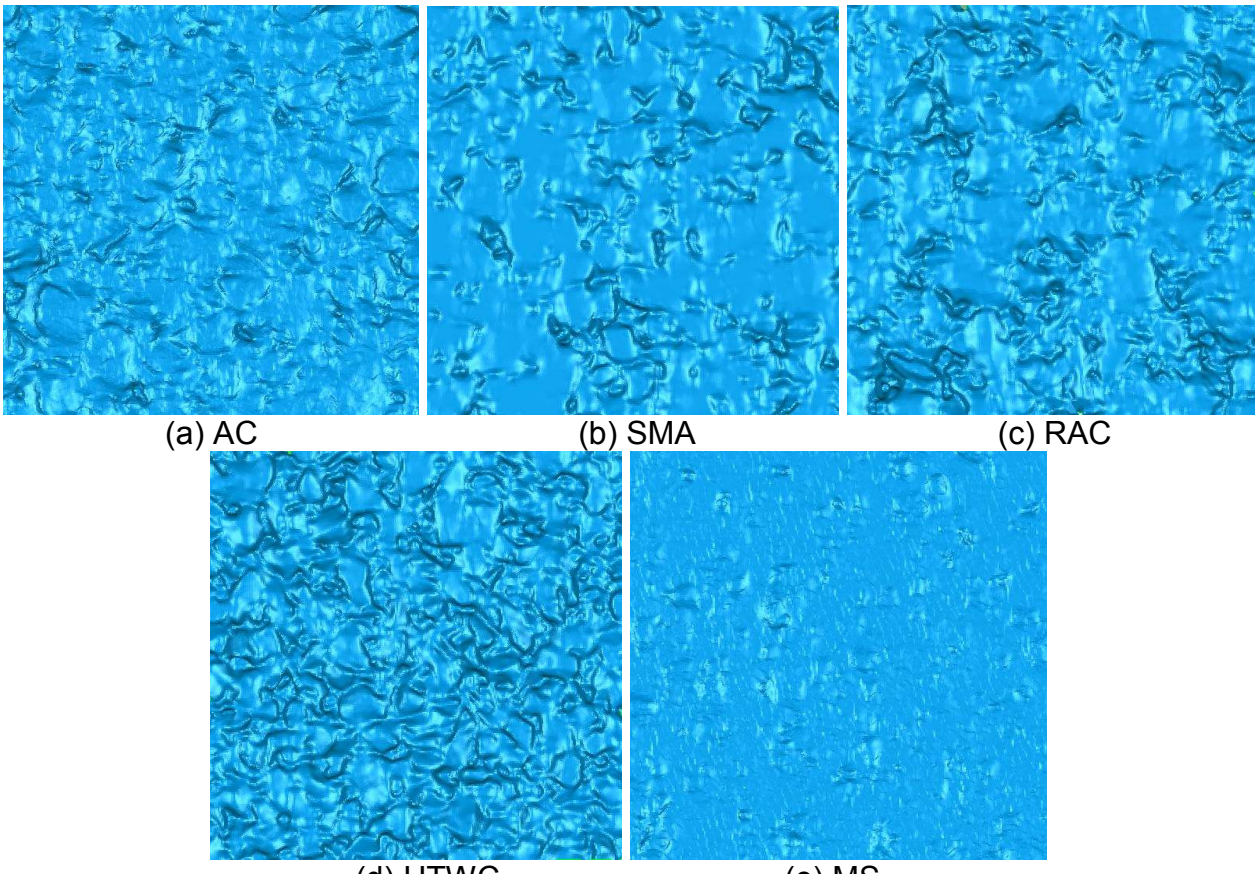

(a) AC (b) SMA (c) RAC

(d) UTWC (e) MS

Figure 1 - Typical 3-D digital macrotextures

3. INDICATORS DESCRIBING 3-D CHARACTERISTICS OF MACROTEXTURE

The original data of the 3-D digital macrotexture are processed using Geomagic Studio 12 before indicators are constructed. Firstly, rotation and transformation actions are conducted to make the XY coordination plane coincident with the fitting plane of the macrotexture, X axis and Y axis parallel to the boundary of the macrotexture respectively, the origin at the centre of the macrotexture, and the Z direction coincident with the normal of the fitting plane of the macrotexture. Then, the original unordered point clouds data of macrotexture are transformed to ordered point clouds with 0.5mm spacing interval at X and Y directions and the unit normal vectors of each point are calculated.

Table 2 - Test results of pavement skid resistance using DFT

ID	DFT60	ID	DFT60	ID	DFT60
G101-MS-1	0.351	G101-UTWC-6	0.479	G111-RAC-6	0.350
G101-MS-2	0.415	G101-SMA-3	0.462	G111-AC-1	0.414
G101-MS-3	0.364	G101-SMA-4	0.406	G111-AC-2	0.423
G101-MS-4	0.401	G101-UTWC-7	0.495	G111-AC-3	0.427
G101-UTWC-1	0.579	G101-SMA-5	0.428	G111-AC-4	0.389
G101-SMA-1	0.402	G101-UTWC-8	0.490	G111-AC-5	0.458
G101-UTWC-2	0.534	G111-RAC-1	0.409	G111-AC-6	0.378
G101-UTWC-3	0.539	G111-RAC-2	0.437	G111-AC-7	0.438
G101-UTWC-4	0.597	G111-RAC-3	0.343	X011-AC-1	0.471
G101-UTWC-5	0.473	G111-RAC-4	0.394	X011-AC-2	0.468
G101-SMA-2	0.503	G111-RAC-5	0.441	X011-AC-3	0.441

According to the processed 3-D digital macrotexture data, three indicators of σ (mm), N_a (rad), and N_{ca} (hereinafter called 3-D macrotexture indicators) are constructed. Equation (1), equation (2), and equation (3) represent the indicators respectively. Table 3 lists the values of the macrotexture indicators.

$$\sigma = \sqrt{\frac{1}{n-1}\sum_{i=1}^{n}(Z_i - \bar{Z})^2} \tag{1}$$

Where: n is the point number in macrotexture data; Z is the value of Z coordination of the point; $\bar{Z}$ is the mean of Z.

$$N_a = \frac{1}{n}\sum_{i=1}^{n}\arccos N_Z^i \tag{2}$$

Where: N_Z is the Z component of the unit normal vector of the point. In fact N_Z is also the cosine value of the angle between the point normal vector and Z axis.

$$N_{ca} = \frac{1}{n}\sum_{i=1}^{n}N_Z^i \tag{3}$$

To evaluate the relationships between the macrotexture indicators and DFT60, correlation analysis is conducted using SAS. The Pearson correlation coefficient matrix of DFT60 and the macrotexture indicators is listed in table 4. The correlation coefficient between σ, derived from the 3-D digital macrotexture, and MTD, derived from the real pavement surface, is 0.92487. It is shown that the method for 3-D digital macrotexture collection is reliable enough. In addition, there is significant improvement in describing pavement macrotexture using N_a and N_{ca} than using MTD for skid resistance evaluation. The correlation coefficients of DFT60-N_a and DFT60-N_{ca} are all above 0.6, while the correlation coefficients of DFT60-MTD is just 0.44832 though the correlation coefficients of MTD-N_a and MTD-N_{ca} are higher.

Table 3 - Indicators of pavement surface macrotexture

ID	MTD/mm	σ/mm	N_a/Rad	N_{ca}
G111-AC-1	0.725	0.447	0.192	0.974
G111-AC-2	0.905	0.538	0.235	0.962
G111-AC-3	0.921	0.514	0.215	0.968
G111-AC-4	0.698	0.554	0.242	0.957
G111-AC-5	0.697	0.577	0.247	0.954
G111-AC-6	0.767	0.436	0.183	0.977
G111-AC-7	0.731	0.498	0.203	0.969
X011-AC-1	0.722	0.474	0.217	0.966
X011-AC-2	0.697	0.361	0.168	0.979
X011-AC-3	0.797	0.499	0.208	0.969
G101-MS-1	0.437	0.180	0.067	0.996
G101-MS-2	0.382	0.258	0.084	0.994
G101-MS-3	0.425	0.176	0.064	0.997
G101-MS-4	0.515	0.249	0.092	0.993
G111-RAC-1	1.056	0.958	0.300	0.938
G111-RAC-2	1.055	0.798	0.271	0.949
G111-RAC-3	0.931	0.791	0.278	0.947
G111-RAC-4	0.969	0.667	0.250	0.954
G111-RAC-5	1.206	0.977	0.307	0.934
G111-RAC-6	1.081	0.815	0.287	0.942
G101-SMA-1	0.714	0.554	0.229	0.958
G101-SMA-2	1.056	0.776	0.298	0.939
G101-SMA-3	1.086	0.917	0.300	0.938
G101-SMA-4	0.848	0.691	0.263	0.951
G101-SMA-5	0.806	0.573	0.225	0.964
G101-UTWC-1	0.982	0.682	0.333	0.929
G101-UTWC-2	0.985	0.757	0.343	0.924
G101-UTWC-3	1.086	0.795	0.379	0.911
G101-UTWC-4	1.119	0.743	0.355	0.921
G101-UTWC-5	0.870	0.515	0.247	0.958
G101-UTWC-6	0.873	0.538	0.245	0.959
G101-UTWC-7	0.919	0.608	0.280	0.948
G101-UTWC-8	0.930	0.615	0.272	0.950

Table 4 - Pearson correlation coefficient matrix of DFT60 and macrotexture indicators

Indicators	DFT60	MTD	σ	N_a	N_{ca}
DFT60	1	0.44832	0.30915	0.60327	-0.60924
MTD	0.44832	1	0.92487	0.91175	-0.88646
σ	0.30915	0.92487	1	0.89565	-0.89362
N_a	0.60327	0.91175	0.89565	1	-0.98434
N_{ca}	-0.60924	-0.88646	-0.89362	-0.98434	1

4. RELATIONSHIP BETWEEN DFT60 AND MACROTEXTURE INDICATORS

To validate the potential advantages of the 3-D macrotexture indicators, the relationship between DFT60 and the macrotexture indicators is analyzed using regression method. Scatter plot matrix is helpful for regression analysis. Figure 2 gives the scatter plot matrix of DFT60 and macrotexture indicators. The plots show complicated relationships between DFT60 and the macrotexture indicators. It is difficult to describe the relationship between DFT60 and macrotexture characteristics just using one macrotexture indicator. So, multiple linear regression analysis with stepwise selection is conducted using SAS. Table 5 lists the stepwise selection result. Three macrotexture indicators, including N_a, σ, and MTD, entered the regression model with R-square of 0.6775. Though MTD finally enters the model, its contribution for R-square is just 0.0315. Equation (4) gives the detailed linear relationship model. Figure 3 is the scatter plot of measured DFT60 and predicted DFT60 using equation (4). The distribution of regression residual is depicted in figure 4.

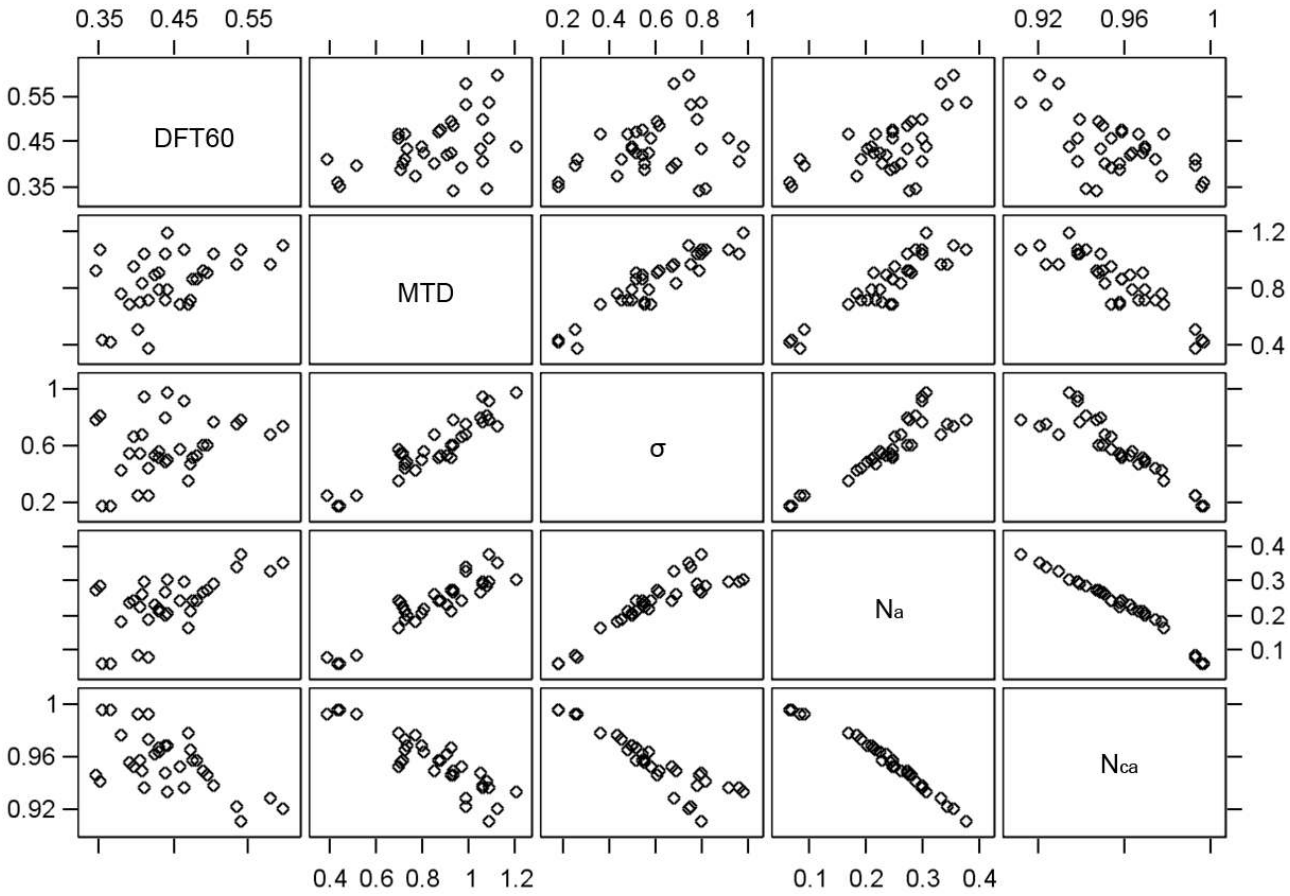

Figure 2 - Scatter plot matrix of DFT60 and macrotexture indicators

Table 5 - Summary of stepwise selection

Step	Variable entered	Partial R-square	Model R-square	C(p)	F value	Pr > F
1	N_{ca}	0.3712	0.3712	26.0675	18.3	0.0002
2	σ	0.2748	0.646	4.0044	23.28	<.0001
3	MTD	0.0316	0.6775	3.2407	2.84	0.1028

$$DFT60 = -4.33086N_{ca} - 0.44673\sigma + 0.14878MTD + 4.72378 \quad (4)$$

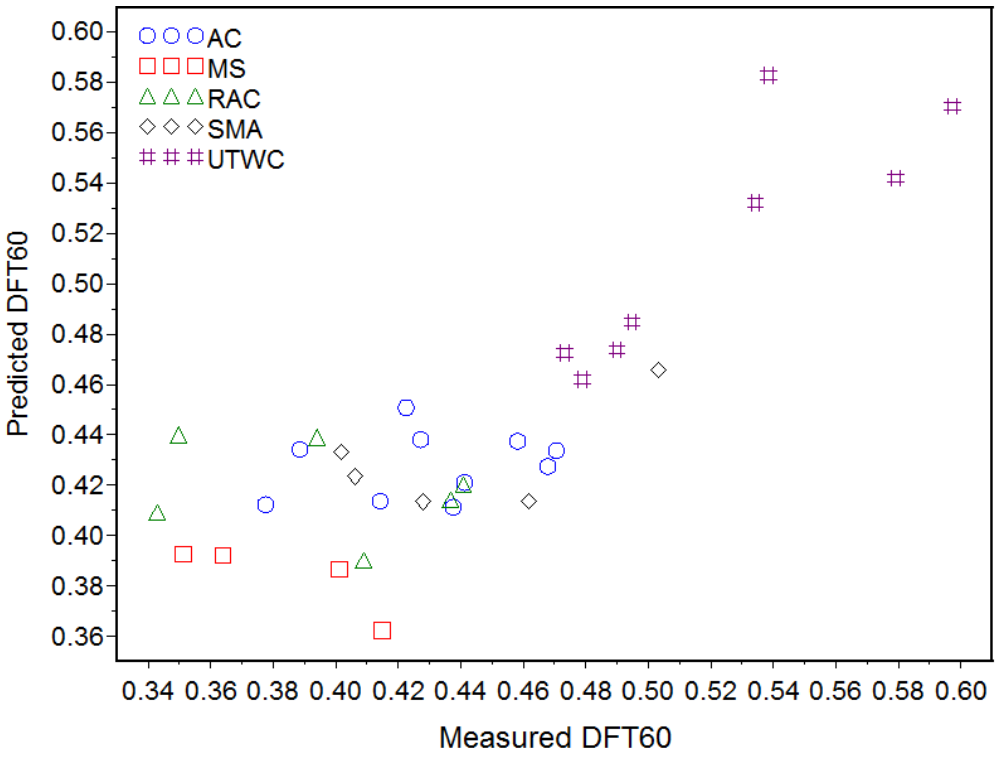

Figure 3 - Scatter plot of measured DFT60 and predicted DFT60 using linear regression

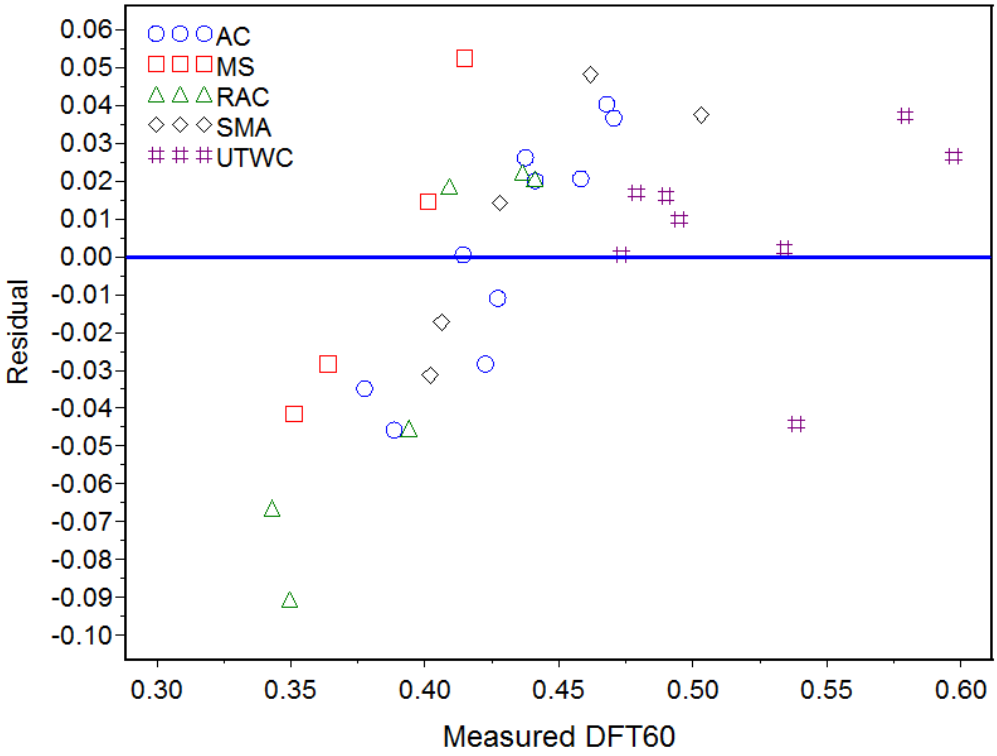

Figure 4 - Scatter plot of measured DFT60 and residual of linear regression

Linear model is obviously not enough to describe the relationship between DFT60 and the macrotexture indicators. This work tries quadratic polynomial regression model as equation (5).

$$DFT60 = MAM^T + BM^T + c \quad (5)$$

Where: A is the coefficient matrix of quadratic terms; B is the coefficient row vector of linear terms; c is a constant; M is the macrotexture indicator row vector.

Table 6, table 7, and table 8 list the R-square and Sum of Squares Error (SSE) when one, two, and three macrotexture indicators enter the quadratic polynomial regression model respectively. When just one macrotexture indicator enters the model, N_a has the highest R-square of 0.4383. When two macrotexture indicators enter the model, the combination of N_a and σ has the highest R-square of 0.7242 with an increase of 0.2859 than the case of one macrotexture indicator. When three macrotexture indicators enter the model, the combination of N_a, σ, and MTD has the highest R-square of 0.7727. MTD just brings an increase of 0.0485 to R-square. Though the regression model will more complicated with more indicators entered, regression residual decreases with more indicators entered. So, this work tries using all four macrotexture indicators in the regression model. Table 9 and table 10 list the significance test parameters and residual of regression with all four macrotexture indicators. In this case, R-square increases to 0.8375. The corresponding values of *A* and *B* are showed in equation (6) and equation (7) respectively and c is -2111.4835 when *M* is [*MTD*, *σ*, N_a, N_{ca}]. Figure 5 is the scatter plot of measured DFT60 and predicted DFT60 using equation (5) with all four macrotexture indicators. The distribution of regression residual is depicted in figure 6.

Table 6 - R-square and SSE when one macrotexture indicator enters the model

Variable entered	MTD	σ	N_a	N_{ca}
R-square	0.2018	0.1853	0.4383	0.4179
SSE	0.0991	0.1011	0.0697	0.0722

Table 7 - R-square and SSE when two macrotexture indicators enter the model

Variables entered	MTD/σ	MTD/N_a	MTD/N_{ca}	σ/N_a	σ/N_{ca}	N_a/N_{ca}
R-square	0.3952	0.5132	0.4892	0.7242	0.6688	0.6088
SSE	0.0751	0.0604	0.0634	0.0342	0.0411	0.0486

Table 8 - R-square and SSE when three macrotexture indicators enter the model

Variable not entered	MTD	σ	N_a	N_{ca}
R-square	0.7810	0.6647	0.7245	0.7727
SSE	0.0272	0.0416	0.0342	0.0282

Table 9 - Significance test parameters of regression with all four macrotexture indicators

Regression	DF	Type I sum of squares of model	R-square	F value	Pr > F
Linear	4	0.0844	0.6803	18.84	<.0001
Quadratic	4	0.0087	0.07	1.94	0.1478
Crossproduct	6	0.0108	0.0873	1.61	0.201
Total model	14	0.1039	0.8375	6.63	0.0002

Table 10 - Residual of regression with all four macrotexture indicators

Residual	DF	Sum of squares	Mean square
Total error	18	0.0202	0.0011

$$A = \begin{bmatrix} -1.4793 & 1.5765 & 12.4349 & 36.3652 \\ 1.5765 & 0.4593 & 2.8052 & 17.0440 \\ 12.4349 & 2.8052 & -229.7726 & -684.3022 \\ 36.3652 & 17.0440 & -684.3022 & -2036.5838 \end{bmatrix} \quad (6)$$

$$B = \begin{bmatrix} -74.8844 & 38.0538 & 1399.2822 & 4148.3951 \end{bmatrix} \quad (7)$$

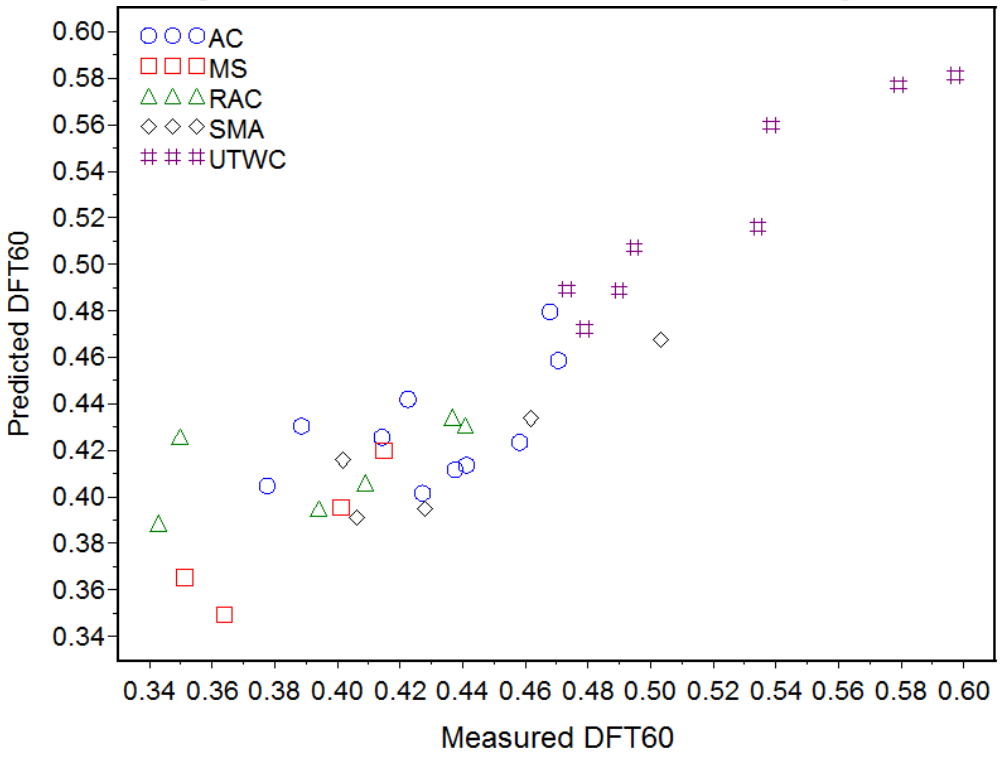

Figure 5 - Scatter plot of measured DFT60 and predicted DFT60 using quadratic polynomial regression with all four macrotexture indicators

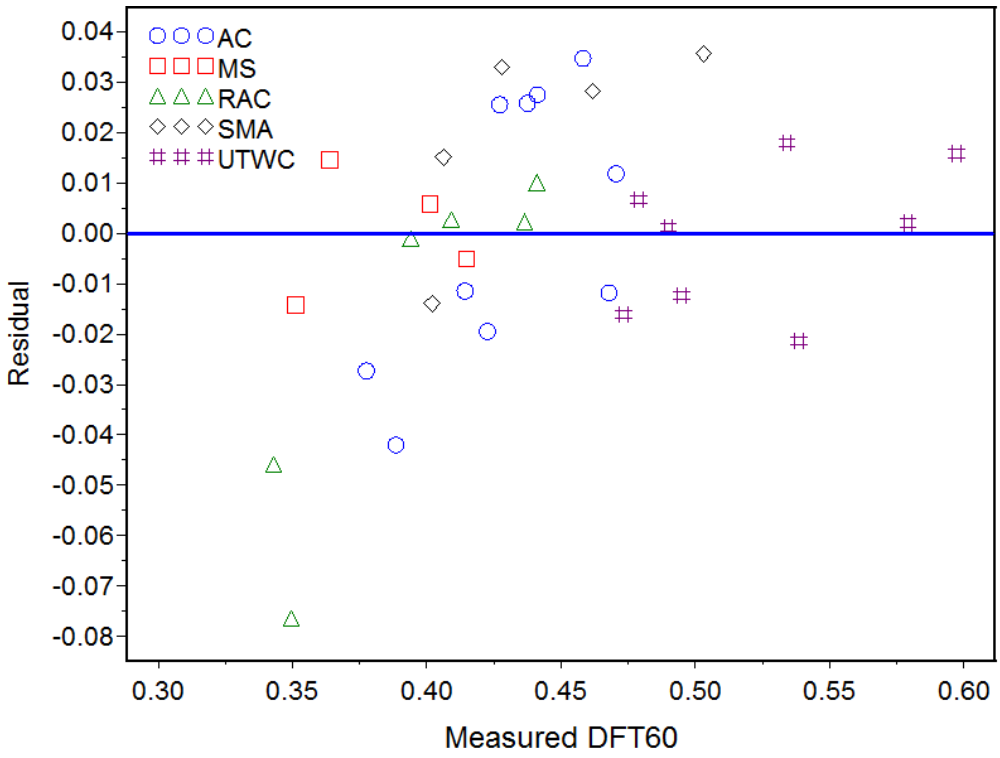

Figure 6 - Scatter plot of measured DFT60 and residual of quadratic polynomial regression with all four macrotexture indicators

The regression analyses show obvious improvement derived from 3-D macrotexture indicators in pavement skid resistance evaluation, though the 3-D macrotexture indicators constructed in this work are not very detailed. But all indicators cannot better describe the relationship between macrotexture and skid resistance alone using linear or quadratic polynomial model. It is concluded that the relationship between macrotexture and skid resistance is so complicated. Another aspect of the problem is each indicator discussed in this work is not detailed enough to describe the characteristics of macrotexture. In addition, both the linear model and the quadratic polynomial model show a certain pavement type dependent according to the figure 3 through figure 6. It is necessary and possible to construct more detailed macrotexture indicators for pavement skid resistance evaluation based on the 3-D digital macrotexture in the future work.

5. CONCLUSIONS

This work tries a method to collect the pavement 3-D digital macrotexture using a 3-D laser scanner for skid resistance evaluation. Field tests are conducted at 33 asphalt pavement test sites with various pavement types and highway grades to validate the collection method and the potential improvement from application of the 3-D digital macrotexture in pavement skid resistance evaluation. The conclusion can be summarized as follows:

1) The method using the 3-D laser scanner adopted in this work can fulfil the requirements of in situ collection of 3-D digital macrotexture.
2) Indicators derived from 3-D digital macrotexture have obvious advantage than TMD for pavement skid resistance evaluation.
3) The quadratic polynomial model with the four indicators is relatively better to describe the relationship between macrotexture and skid resistance.

This work is just a preliminary evaluation. Further analysis and validation is recommended prior to the widespread use of this procedure in practice:

1) More detailed indicators should be constructed based on the 3-D digital macrotexture with consideration of the mechanism of tire-pavement friction.
2) Simpler model describing the relationship between macrotexture and skid resistance should be studied for practice application.

ACKNOWLEDGEMENT

The research reported in this paper is funded by the National Natural Science Foundation of China (50908004).

REFERENCES

1. Henry, J. J. (2000). Evaluation of pavement friction of characteristics. NCHRP Synthesis 291. Washington D.C., Transportation Research Board, National Research Council
2. Wambold, J. C., Antle, C. E., Henry, J. J., Rado, Z. (1995). International piarc experiment to compare and harmonize texture and skid resistance measurements. Paris, Permanent International Association of Road Congresses
3. ASTM (2006). Standard terminology relating to vehicle-pavement systems. pp10
4. Stroup-Gardiner, M., Studdard, J., Wagner, C. (2004). Evaluation of hot mix asphalt

macro- and microtexture. Journal of Testing and Evaluation.Vol32, No1, pp1-10
5. Ergun, M., Iyinam, S., Iyinam, A. F. (2005). Prediction of road surface friction coefficient using only macro- and microtexture measurements. Journal of Transportation Engineering.Vol131, No4, pp311-319
6. Gunaratne, M., Bandara, N., Medzorian, J., Chawla, M., Ulrich, P. (2000). Correlation of tire wear and friction to texture of concrete pavements. Journal of Materials in Civil Engineering.Vol12, No1, pp46-54
7. Panagouli, K., Kokkalis, A. G. (1998). Skid resistance and fractal structure of pavement surface. Chaos, Solitons & Fractals.Vol9, No3, pp493-505
8. Zhao, Z. (2005). Reseacrh on skid resistance technology of asphalt pavement based on fractal method. Xi'an, Chang'an University
9. Huang, C. (2002). Mathematical characterization of road surface texture and its relation to laboratory friction measures. Houghton, Michigan Technological University
10. Wang, D., Li, W., Zhang, X. (2004). Evaluation and Measurement of Asphalt Pavement Surface Texture Depth with Digital Image Technique. Journal of South China University of Technology (Natural Science Edition). Vol32, No2, pp42-45